Fusion Engineering and Design xxx (2014) xxx–xxx

Contents lists available at ScienceDirect

Fusion Engineering and Design

journal homepage: www.elsevier.com/locate/fusengdes

The dynomak: An advanced spheromak reactor concept with imposed-dynamo current drive and next-generation nuclear power technologies

D.A. Sutherland*, T.R. Jarboe, K.D. Morgan, M. Pfaff, E.S. Lavine, Y. Kamikawa, M. Hughes, P. Andrist, G. Marklin, B.A. Nelson

University of Washington, AERB Room 120, Box 352250, Seattle, WA 98105-2250, USA

ARTICLE INFO

Article history:
Received 25 June 2013
Received in revised form 24 March 2014
Accepted 25 March 2014
Available online xxx

Keywords:
Spheromak
Helicity
Current drive
Reactor concept
Economics

ABSTRACT

A high-β spheromak reactor concept has been formulated with an estimated overnight capital cost that is competitive with conventional power sources. This reactor concept utilizes recently discovered imposed-dynamo current drive (IDCD) and a molten salt (FLiBe) blanket system for first wall cooling, neutron moderation and tritium breeding. Currently available materials and ITER-developed cryogenic pumping systems were implemented in this concept from the basis of technological feasibility. A tritium breeding ratio (TBR) of greater than 1.1 has been calculated using a Monte Carlo N-Particle (MCNP5) neutron transport simulation. High temperature superconducting tapes (YBCO) were used for the equilibrium coil set, substantially reducing the recirculating power fraction when compared to previous spheromak reactor studies. Using zirconium hydride for neutron shielding, a limiting equilibrium coil lifetime of at least thirty full-power years has been achieved. The primary FLiBe loop was coupled to a supercritical carbon dioxide Brayton cycle due to attractive economics and high thermal efficiencies. With these advancements, an electrical output of 1000 MW from a thermal output of 2486 MW was achieved, yielding an overall plant efficiency of approximately 40%.

1. Motivation

An advanced spheromak reactor concept, henceforth called the dynomak, was formed around the recently discovered imposed-dynamo current drive (IDCD) mechanism on the steady, inductive, helicity injected torus (HIT-SI) experiment at the University of Washington. As opposed to other dynamo driven spheromak and reversed-field pinch (RFP) experiments that rely on driving the configuration unstable to provide cross-field current drive, IDCD perturbs and drives a stable spheromak configuration, possibly avoiding the severe confinement quality limitations present in other dynamo driven experiments [1]. Additionally, it has been suggested that this mechanism could provide plasma current profile control by tuning the imposed magnetic fluctuation profile via appropriate phasing of multiple inductive helicity injectors [1]. Lack of profile control has been suggested to be one of the main initiators of disruptions in tokamaks, and thus IDCD-enabled profile control could prove invaluable for tokamak reactor concepts as well [1]. Also, conventional current drive methods, namely neutral beam injection (NBI) and radiofrequency (RF) current drive, are inefficient when compared to the possible efficiency of IDCD [1]. With an efficient current drive scheme like IDCD, a lower bootstrap fraction tokamak or a spheromak configuration could be realized with a reasonable recirculating power fraction. It should be noted that the IDCD mechanism and the extrapolations from the university-scale experiment HIT-SI to the reactor-scale dynomak are speculative. In particular, core current drive via helicity injection in larger devices must be experimentally verified for IDCD to be considered a complete current drive solution for a fusion system; current drive within the core of a reactor-relevant plasma via IDCD has not been demonstrated. However, this study seeks to develop a vision for an IDCD-enabled fusion reactor system under the assumption that this current drive mechanism scales to reactor relevant regimes, providing sufficient current drive to maintain a constant $\lambda \equiv \frac{\mu_0 j}{B}$ profile within the last closed flux surface. IDCD will be used in this study to sustain a spheromak equilibrium with an ensemble of inductive helicity injectors.

A guiding philosophy behind this reactor concept was engineering simplicity and attractive reactor economics, and thus a spheromak configuration was chosen in an effort to minimize

* Corresponding author. Tel.: +1 206 5436133.
E-mail address: das1990@uw.edu (D.A. Sutherland).

http://dx.doi.org/10.1016/j.fusengdes.2014.03.072
0920-3796/

superconducting coil set requirements. This choice of configuration provided a more compact, low-aspect-ratio reactor concept (A = 1.5) when compared to typical tokamak and stellarator configurations [2]. Externally linked toroidal configurations suffer from compact size limitations partly dictated by the inboard $j \times B$ stress approaching unmanageable limits should high fields be used to approach economically attractive fusion power densities. Additionally, the inboard fast neutron flux limits the superconducting coil lifetime unless substantial neutron shielding is used, which typically comes at the expense of tritium breeding blanket materials. Without sufficient tritium breeding materials, an increase in reactor size is typically required to simultaneously achieve a sufficient TBR and an economical superconducting coil set lifetime. However, the simply connected spheromak topology and reliance on plasma currents to generate toroidal magnetic flux eliminates the mentioned structural and nuclear engineering limitations intrinsic to tokamaks and stellarators, allowing for the possibility of more compact, cost effective reactors.

Previous spheromak reactor concepts exploited high-β ($\beta \equiv (2\mu_o p)/B^2$) plasmas in very compact configurations with neutron wall loadings upwards of 20 MW m^{-2} for a proposed 1 GWe power plant [3], which are aggressive values when compared to more recent fusion reactor design studies [2,4] that benefit from a more substantive understanding of damage to materials in a deuterium-tritium (DT) fusion environment. Additionally, electrodes were used to inject helicity for spheromak sustainment in the aforementioned study, which results in open field lines that are effectively line-tied to the electrodes. Thus, this method of helicity injection effectively introduces a diverted magnetic topology [3], which is characteristic of most modern tokamaks that exploit H-mode. However, the use of a diverted topology focuses the plasma heat load, when it would be preferred from a materials engineering and first wall cooling standpoint to distribute the heat load uniformly on the plasma-facing first wall. The dynomak reactor system eliminates the necessity for a diverted topology using steady inductive helicity injection by not requiring electrodes. Thus, it is argued the plasma heat load will be distributed uniformly on the first wall, eliminating aggressive divertor cooling requirements.

While considering the economic attractiveness of fusion power, the ARIES-AT reactor study found that for 1 GWe power plants, economic improvements begin to saturate for increasing neutron wall loadings above approximately 4 MW m^{-2} [4]. While considering first wall cooling requirements using a uniform plasma heat load for the dynomak reactor concept, a neutron wall loading of 4.2 MW m^{-2} was chosen as an operating point. This low neutron wall loading, when compared to the previously mentioned spheromak reactor study [3], equates to a longer fusion power core (FPC) lifetime while optimizing reactor economics using the wall loading metric from the ARIES-AT study. It is an economic imperative for fusion energy to be competitive with conventional power sources to be considered as a replacement. The estimated overnight capital cost of the dynomak reactor concept will be argued to be competitive with fossil fuel energy sources. Using established materials will allow for an expedited NRC licensing process with a well developed pedigree of material performance in fission reactors; however, a fusion nuclear science facility (FNSF) will still be required. An FNSF is a necessary developmental step to study material degradation in a DT fusion environment and first wall plasma-material interactions. Lastly, it was sought to minimize the activation of surrounding reactor components to fully exploit one of the main advantages of fusion over fission: having only limited quantities of short-lived radioactive waste dependent on the choice of surrounding materials.

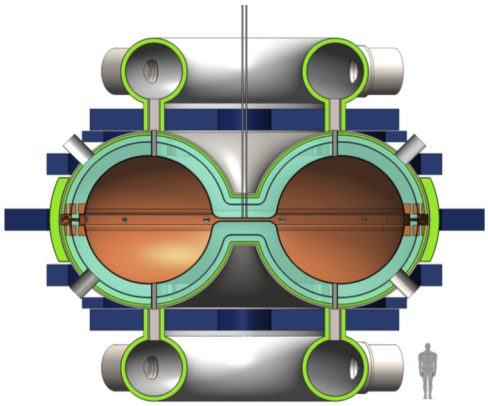

Fig. 1. A sliced rendering of the dynomak reactor concept, excluding the secondary power conversion cycle.

2. Dynomak overview

The dynomak is a high-β spheromak reactor concept that uses six inductive helicity injectors located on the outboard midplane to sustain a spheromak equilibrium with a nearly circular poloidal cross section. A molten salt mixture of LiF and BeF_2 commonly referred to as FLiBe is used as the first wall coolant, neutron moderator and tritium breeding medium [15]. The widespread usage of FLiBe is motivated by the engineering simplicity of using a single working fluid in the blanket system. A dual-chambered blanket system is used in the dynomak concept, which is depicted in turquoise in Fig. 1, and will be described in detail. The FLiBe exits the dynomak reactor through the depicted large pipes and couples to the secondary, supercritical CO_2 power conversion cycle.

The orange copper coils located near the outboard midplane in Fig. 1 exclude magnetic flux from the helicity injector region to ensure satisfactory injector operation. Due to the loss of blanket material in this region, an additional zirconium hydride neutron shield is placed in the outboard midplane region to supplement the zirconium hydride shield encircling the nearly doubly connected reactor vessel topology. Neutron shielding is depicted in green in Fig. 1. An insulating break is placed on the geometric axis on midplane, classifying this system as a spheromak and allowing for free creation of toroidal flux. Gas injection occurs in the insulating break region, which will expand major radially outward to fuel the reactor. Pumping channels on top and bottom are used to remove helium ash in an effort to maintain a helium fraction of less than 3%. Two, large pumping manifolds on top and bottom are depicted with ITER-developed cryosorption pumps oriented to avoid fast neutron beams emanating from the pumping channels. The high-temperature superconducting equilibrium coil set is depicted in blue, which utilizes yttrium barium copper oxide (YBCO) tapes operating at subcooled liquid nitrogen temperatures of approximately 65 K. This choice of superconducting material reduces the cooling power requirement when compared to more conventional niobium based superconductors that typically require liquid helium cooling. YBCO has been tested up to a fluence of 2.8×10^{22} m^{-2} at a temperature of 81 K, and no degradation of the critical current density was observed [5]. The threshold fast neutron fluence for the degradation of the critical current density of Nb_3Sn is approximately 3×10^{22} m^{-2}, and thus YBCO irradiation resistance may be as good or better than Nb_3Sn [5]. A higher tolerance to fast neutron damage of these superconductors would equate to a longer lifetime of these expensive components.

Please cite this article in press as: D.A. Sutherland, et al., The dynomak: An advanced spheromak reactor concept with imposed-dynamo current drive and next-generation nuclear power technologies, Fusion Eng. Des. (2014), http://dx.doi.org/10.1016/j.fusengdes.2014.03.072

Table 1
Key parameters of the dynomak reactor operating point.

Parameter	Symbol	Value
Major radius [m]	R_o	3.75
Minor radius [m]	a	2.5
Toroidal plasma current [MA]	I_p	41.7
Number density ($\times 10^{20}$ m^{-3})	n_e	1.52
Wall-averaged β (%)	$\langle\beta_{\text{wall}}\rangle$	16.6
Peak temperature (keV)	T_e	20
Neutron wall loading (MW m^{-2})	P_n	4.2
First wall heat flux (MW m^{-2})	q''	1.05
Helicity injector power (MW)	P_{CD}	58.5
FLiBe inlet temperature (°C)	T_{in}	480
FLiBe inlet temperature (°C)	T_{out}	580
Global blanket flow rate (m^3 s^{-1})	$\dot{U}$	5.17
Thermal power (MW)	P_{th}	2486
Fusion power (MW)	P_{fus}	1953
Electrical power (MW)	P_e	1000
Plasma gain	Q_p	33
Engineering gain	Q_e	9.5
Thermal efficiency (%)	η_{th}	≥45
Global efficiency (%)	η	≥40

2.1. Operating point

The key parameters of interest of the dynomak reactor concept are provided in Table 1. Note that the value for $\langle\beta_{\text{wall}}\rangle$ presented in Table 1 is the root-mean-square average of the local beta β_{wall} over the plasma volume. The relations in Eqs. (2) and (3) provide these definitions of β in both forms, along with the calculation of the magnetic field at the wall B_{wall} in Eq. (1).

$$B_{\text{wall}} = \frac{\mu_o I_p}{2\pi a} \tag{1}$$

$$\beta_{\text{wall}} = \frac{2\mu_o p}{B_{\text{wall}}^2} \tag{2}$$

$$\langle\beta_{\text{wall}}\rangle \equiv \sqrt{\frac{\int \beta_{\text{wall}}^2 \, dV}{2\pi^2 R_o a^2}} \tag{3}$$

With the key parameters for the dynomak operating point provided, subsequent sections will provide details concerning particular subsystems of interest. First, the spheromak core concept will be presented, which will include the enhanced Grad–Shafranov code calculation that provides the required currents in a prescribed superconducting coil set to provide force balance, and also in the copper coils to ensure desired helicity injector operation. Additionally, the feedback control system, the pumping systems to remove helium ash, and the helicity injector requirements will be discussed.

Second, the multipurpose blanket system will be presented, including the first wall cooling assembly and tritium breeding calculations from MCNP5 neutron transport simulations. A discussion concerning hydrofluoric acid generation, neutralization and erosion concerns for quickly flowing FLiBe in the first wall cooling system will also be provided. A description of the secondary cycle used for power conversion will be given, including the choice of using a supercritical CO_2 Brayton cycle to couple to the primary FLiBe loop. Also, a calculation of the plasma gain Q_p, and, more importantly, the engineering gain Q_e is provided, which is used as a figure of merit for power plant attractiveness. Furthermore, a cost analysis of the dynomak reactor concept will be presented and argued to be competitive with conventional power sources. Lastly, future research requirements to prove IDCD is a feasible method for sustaining a reactor-relevant spheromak configuration and a development path towards a dynomak pilot plant are discussed.

3. The spheromak core concept

3.1. Equilbrium

A stepped λ current profile is imposed in the dynomak reactor concept, with one value of λ being that of the helicity injectors outside the separatrix, and the other value of λ required for current amplification inside the separatrix. This profile is motivated by recent, encouraging toroidal current amplification results on the HIT-SI device [35]. It is again noted that a flat-λ profile throughout the region inside the separatrix suggests core current drive via the IDCD mechanism, which is speculative on reactor scale devices, though is assumed for this study. The profile is robust because it is maintained by keeping fluctuations inside the separatrix above the required value for IDCD. Since the toroidal current gain of this reactor is large (≈1230), virtually the entire plasma volume will be inside the separatrix. An enhanced Grad–Shafranov equilibrium code imposed marginal Mercier stability on each flux surface with a $\lambda a = 2.4$ with an aspect ratio of 1.5. This code provides the necessary currents in a prescribed superconducting equilibrium coil set, and in the outboard midplane copper coils required for flux exclusion from the helicity injector region. The latter coil set is prescribed purely to ensure proper injector operation, and due to the location in the blanket, is chosen to be copper instead of YBCO due to the high fast neutron population expected in that region of the blanket. The Grad–Shafranov equilibrium with the corresponding coil set and required currents is presented in Fig. 2.

3.2. Feedback

It was suggested the IDCD mechanism may provide plasma current profile control and thus could largely eliminate this source of disruptions that is observed in tokamak configurations [1]. However, feedback is still required to maintain desired flux surface locations and ensure operation at desired plasma parameters. Because the edge is driven by the six inductive helicity injectors, a diffuse scrape off layer is expected, estimated to be a few centimeters in thickness. As seen in the Grad–Shafranov equilibrium in Fig. 2, it is desired to have a limited plasma with a nearly circular poloidal cross section, requiring approximately 10–20 mm accuracy in flux surface position. The YBCO equilibrium coils will be feedback controlled to keep the plasma at the desired distance from the wall at all times. This method of feedback was successfully implemented on the HIT-II machine at the University of Washington [6]. Flux loops at the positions of the red dots on the flux conserver in Fig. 2 will be the sensors for feedback control of the switching power amplifiers (SPAs). The response time depends on the voltage V_{spa} and current I_{spa} capabilities of the SPA. For a fixed quantity of conductor, the fastest time response is achieved by using the minimum number of turns N_{spa} that still allows the SPAs to supply the required ampere-turns, I_{AT}. Thus, $N = I_{AT}/N_{\text{spa}}I_{\text{spa}}$ and, ignoring resistance in the superconducting coils, $d\psi/dt = V/N$ or,

$$\tau_{\text{resp}} = \frac{I_{AT}\psi}{N_{\text{spa}} I_{\text{spa}} V_{\text{spa}}} \tag{4}$$

where ψ is the flux between the coil and the flux conserver. Using the HIT-SI SPAs (which were also used for costing estimates of the feedback system that will be presented later) yields $I_{\text{spa}} = 800$ A and $V_{\text{spa}} = 800$ V. To ensure a stable equilibrium is maintained, the feedback control system must be capable of raising the external B-field faster than the resistive wall mode instability raises the internal B-field at the flux conserver position. The growth time of the mode is approximately the flux loss time of the flux conserver. Estimating the flux as that of a cylinder with uniform current density inside,

Please cite this article in press as: D.A. Sutherland, et al., The dynomak: An advanced spheromak reactor concept with imposed-dynamo current drive and next-generation nuclear power technologies, Fusion Eng. Des. (2014), http://dx.doi.org/10.1016/j.fusengdes.2014.03.072

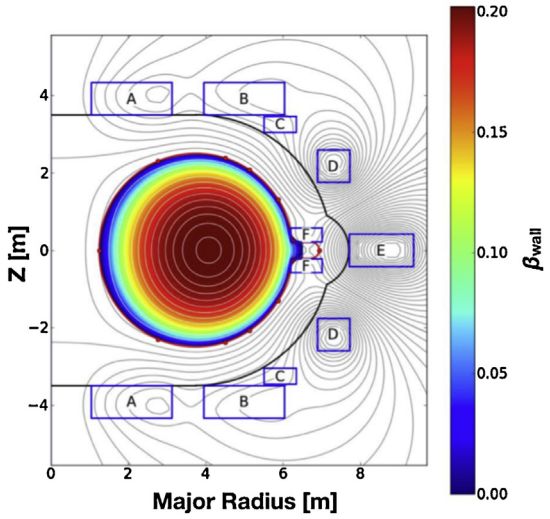

Coil Set	MA-turns
A	-16.3
B	-5.2
C	0.4
D	-11
E	16.8
F	2.6

Fig. 2. Grad–Shafranov equilibrium with corresponding coil set and currents.

and provided with a return current in the wall, yields a flux loss time of

$$\tau_{fl} = \frac{\mu_o a \delta}{2\eta} \tag{5}$$

where a is the minor radius of the device, and δ and η are the thickness and resistivity of the flux conserver, respectively. Given the 10 mm thickness of the flux conserver used in this concept, the flux loss time is estimated to be $\tau_{fl} = 0.93$ s. Thus, it is necessary to provide feedback on a time scale below this estimated flux loss time; a response time of 0.8 s was chosen to allow for a margin of safety.

3.3. Current drive

3.3.1. Requirements

The spheromak magnetic equilibrium is generated by both toroidal and poloidal plasma currents, and will decay due to the finite resistivity of the plasma if some method of sustainment is not employed. As was mentioned previously, six inductive helicity injectors will be used to sustain the spheromak equilibrium via the IDCD mechanism, and an estimation for the current drive power requirements can be obtained from power balance considerations and calculated power coupling efficiencies. The current drive power requirements for the dynomak reactor concept will be strongly dependent on the temperature profile, which sets a Spitzer resistivity profile with $\eta \propto T_e^{-3/2}$. The pressure profile calculated by the enhanced Grad–Shafranov equilibrium code in Fig. 3 was used to numerically calculate the Ohmic power dissipation for the system while assuming a constant density profile with a magnitude of the desired volume averaged density listed in Table 1, for simplicity. The large pressure gradients apparent in Fig. 3 suggest good energy confinement. Core confinement approaching L-mode quality in tokamaks has been observed in decaying spheromaks, namely in the SSPX experiment at LLNL [7]. However, since this device relied on driving the equilibrium unstable to provide current drive, it is reasonable to assume that a sustained stable equilibrium could allow for better confinement than has been previously observed in spheromaks.

The pressure profile provided in Fig. 3 yields an Ohmic power dissipation that is very sensitive to the separatrix temperature, as shown in Fig. 4. The desired separatrix temperature is determined

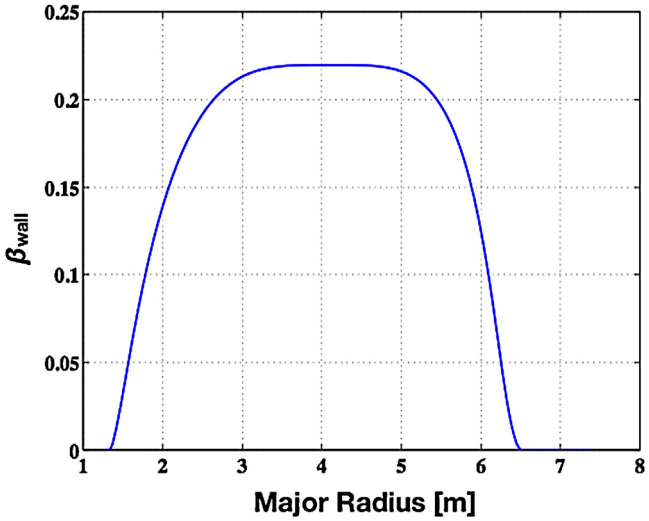

Fig. 3. Major radial pressure profile normalized to the magnetic pressure at the wall ($r = a$) for a midplane slice of the constant F' (constant j/B) Grad–Shafranov equilibrium that imposes marginal Mercier stability on each flux surface for p'.

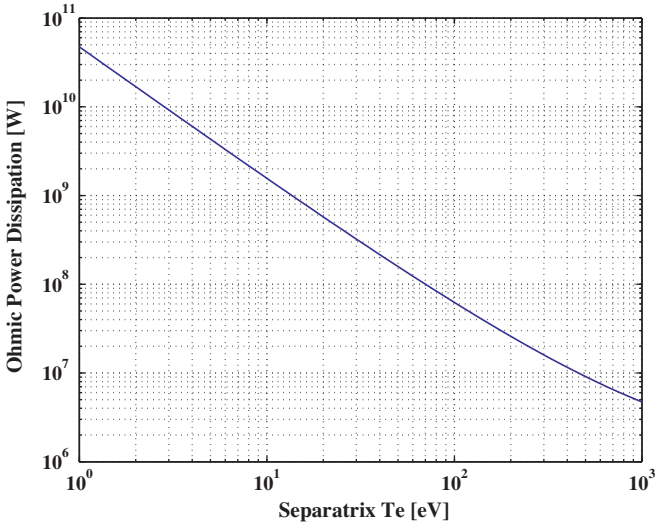

Fig. 4. The global Ohmic power dissipation versus separatrix temperature for the dynomak reactor concept. Note this calculation includes the contribution from the poloidal plasma current.

Please cite this article in press as: D.A. Sutherland, et al., The dynomak: An advanced spheromak reactor concept with imposed-dynamo current drive and next-generation nuclear power technologies, Fusion Eng. Des. (2014), http://dx.doi.org/10.1016/j.fusengdes.2014.03.072

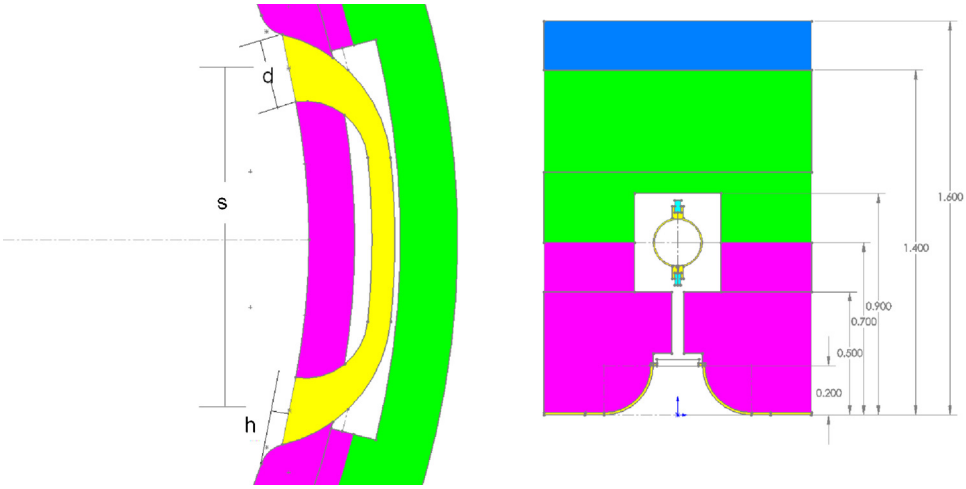

Fig. 5. A depiction of the helicity injectors from toroidal (left) and poloidal (right) perspectives. To the left is a midplane cross section showing the toroidal extent of an injector, showing the free parameters to vary for optimization: the spacing between injector mouths *s*, the inside diameter of an injector mouth *d*, and the offset of the mouth from the first wall *h*. To the right is a poloidal cross section cut down the center of an injector for the dimensions listed. The FLiBe blanket is magenta, the first wall structure in yellow, the ZrO_2 ceramic in teal, the ZrH_2 shield in green, and the equilibrium coil in blue. A vacuum chamber surrounds the injector to provide enough room for the coils. (For interpretation of the references to color in this figure legend, the reader is referred to the web version of the article.)

by economic considerations, namely, the acceptable recirculating power fraction that is dominated by the IDCD power requirements, which will be discussed in detail with the plasma gain Q_p and engineering gain Q_e calculations. Typical separatrix temperatures of 100 - 300 eV have been observed to be fairly consistent across high-performance tokamak devices, and thus a separatrix temperature of 200 eV is assumed for calculations of the current drive power requirement [11]. This would equate to an Ohmic power dissipation of approximately 24 MW as seen in Fig. 4. Provided a 41% coupling efficiency from the IDCD equation [1], and a 80% wall plug efficiency that seems reasonable from an unoptimized 70% achieved on the HIT-SI device, yields a current drive power requirement of 73 MWe for the dynomak reactor with a 200 eV separatrix.

3.3.2. Helicity injectors

The coupled current drive power requirement is 58.5 MW assuming a 41% coupling efficiency calculated for the IDCD mechanism. The required injector currents can be found using the IDCD provided by Eq. (6),

$$\dot{I}_{\mathrm{tor}} + \frac{I_{\mathrm{tor}}}{\tau_{L/R}} = \frac{C_1}{8\pi a^3 ne} I_{\mathrm{inj}}^2 \tag{6}$$

where I_{tor} is the toroidal plasma current, $\tau_{L/R}$ is the characteristic L/R time derived from helicity balance, C_1 is a geometrical fitting parameter equal to 0.94, and I_{inj} is the injector current [1]. To find the steady-state injector current requirement for sustainment via the IDCD mechanism, $\dot{I}_{\mathrm{tor}} \to 0$ and rearrangement leads to Eq. (7),

$$I_{\mathrm{inj}} = \sqrt{\frac{8\pi a^3 ne}{C_1 \tau_{L/R}}} I_{\mathrm{tor}} \tag{7}$$

From the dynomak operating point in Table 1, the volume averaged density is $n = 1.52 \times 10^{20}\ \mathrm{m}^{-3}$, the toroidal plasma current is $I_{\mathrm{tor}} = 41.7$ MA, and the L/R time is estimated to be approximately 340 s. Solving for the injector current requirement I_{inj} for sustaining the dynomak equilibrium yields 35.3 kA. The six inductive helicity injectors used for sustainment are located in the outboard midplane region of the dynomak reactor, as shown in Fig. 1. There is not an abundance of space for the injectors in this region, primarily due to the pull coil (coil E in Fig. 2) that works with the FLiBe-cooled copper coils to exclude flux from the injector region, and helps maintain the desired flux surface positions. Additionally, it is desired to minimize the volume for the helicity injector assemblies that would otherwise be filled with FLiBe in an effort to maximize the tritium breeding ratio (TBR). Thus, size limitations on the helicity injectors constrains the parameter space of possible injector configurations. Fig. 5 depicts the injector geometry that shows the constraining blanket modules described.

Table 2
Properties of yttrium-stabilized zirconium dioxide [ZrO_2–Y_2O_3]. The low coefficient of friction along with the high Young's modulus make it the ideal ceramic insulator to use to hold vacuum on the insulating gap in the injector. As the copper undergoes thermal expansion, the zirconium will slide into the desired placement.

Parameter	Value
Coefficient of friction	0.18
Electrical resistivity (Ω m)	10^{10}
Mass density (kg m^{-3})	6050
Young's modulus (MPa)	2.05×10^5

The first limitation on the injector parameters is the distance away from the confinement volume it can extend. The primary reasons for imposing this limitation are to reduce the current required in the midplane equilibrium coil and allow for sufficient neutron shielding to ensure economical YBCO superconducting tape lifetimes. The closest the equilibrium coil can be to the confinement volume is 50 cm from the maximum major radial location of the injector, which is dictated by the shielding capabilities of ZrH_2 for a limiting, unmoderated fast neutron beam emanating from an injector mouth. Thus, the injector was constrained to not exceed 90 cm past the first wall to optimize fast neutron attenuation by neutron shielding and keeping the midplane equilibrium coil current requirement to a reasonable level.

The next requirement is that the injector must have an insulating gap to allow flux penetration through the copper, but also must hold a vacuum seal between the blanket and the plasma. A ceramic is an ideal choice of material; however, satisfactory high temperature operation with sufficient strength is also required. The ceramic must have a low coefficient of friction to allow for sliding as the surrounding metals expand due to temperature increases, and also be able to maintain a vacuum. For this reason, yttrium stabilized zirconium was selected with pertinent properties listed in Table 2 [12].

A calculation provided the required magnetic fluctuation $B_\perp^2$ profile and an example injector imposed profile for a set of geometric parameters, as shown in Fig. 6. This profile could be further

Please cite this article in press as: D.A. Sutherland, et al., The dynomak: An advanced spheromak reactor concept with imposed-dynamo current drive and next-generation nuclear power technologies, Fusion Eng. Des. (2014), http://dx.doi.org/10.1016/j.fusengdes.2014.03.072

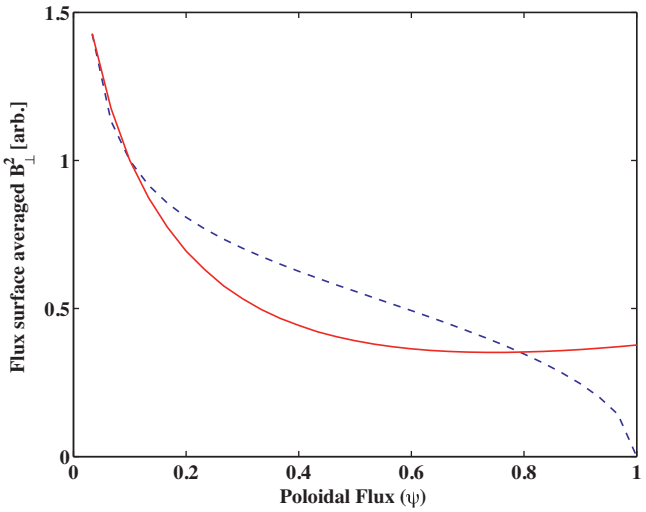

Fig. 6. A representative calculation showing the capability to optimize the magnetic fluctuation profile required for current drive. The required (dashed blue) and applied (solid red) $B_\perp^2(\psi)$ with an injector configuration of the following properties: $s = 3$ m, $d = 1.2$ m, $h = 0.0$ m. Scans over injector parameter space will enable applied profile optimization by minimizing deviations from the required magnetic fluctuation profile. Note that poloidal flux of 1 indicates the location of the magnetic axis. (For interpretation of the references to color in this figure legend, the reader is referred to the web version of the article.)

optimized by varying injector parameters. While using six, evenly spaced injectors around the confinement volume, asymmetrically imposed fluctuations may allow for externally controlled plasma rotation, which could stabilize against resistive wall modes and serve as a global stabilizing feature of the system. Asymmetrically imposed fluctuations can be accomplished by dividing the injectors into three pairs and amplitude modulating the loop voltage supplied to the injectors by appropriately chosen phases. The grouping of injectors into pairs enables constant helicity injection, where each pair consists of injectors 90° out of phase, such that the helicity injection rate $\dot{K} = 2(V_1\psi_1 + V_2\psi_2) = 2V_0\psi_0(\sin^2(\omega_i t) + \cos^2(\omega_i t)) = 2V_0\psi_0$. The resulting loop voltage as a function of time for each injector is provided in Table 3, with ω_i being the injector frequency, ω_r the rotation frequency, and C a constant to be determined from an optimization of providing sufficiency large asymmetries to drive bulk plasma rotation while minimizing injector power coupling inefficiencies.

With these constraints, the injector parameter space must be explored with different experiments and via simulations to determine an optimal injector configuration. HIT-SI3, an upgrade of HIT-SI, has three injectors on one side of the torus that will allow exploration of plasma rotation control with helicity injectors. HIT-SI3 is depicted in Fig. 7, and is beginning operations. A future Proof-of-Principle (PoP) experiment is necessary for experimentally determining the implications of moving injectors to the outboard midplane instead of being located on one side of the machine. Additionally, a PoP experiment is required to confirm that IDCD provides sufficient current drive throughout the region inside the separatrix in reactor relevant plasmas.

Table 3
The applied voltage profiles to each injector to induce an driven asymmetry that rotates around the confinement volume, which should drive a bulk plasma rotation that is favorable for stability and resistive wall mode stabilization.

Injector voltage waveforms
$V_1 = V_0\cos(\omega_i t)[1 - C\cos(\omega_r t)]$
$V_2 = V_0\sin(\omega_i t)[1 - C\cos(\omega_r t)]$
$V_3 = V_0\,cos(\omega_i t)\left[1 - C\,\cos\left(\omega_r t + \frac{2\pi}{3}\right)\right]$
$V_4 = V_0\,sin(\omega_i t)\left[1 - C\,\cos\left(\omega_r t + \frac{2\pi}{3}\right)\right]$
$V_5 = V_0\,cos(\omega_i t)\left[1 - C\,\cos\left(\omega_r t + \frac{4\pi}{3}\right)\right]$
$V_6 = V_0\,sin(\omega_i t)\left[1 - C\,\cos\left(\omega_r t + \frac{4\pi}{3}\right)\right]$

Fig. 7. The new HIT-SI3 experiment that is beginning operations. The three coplanar helicity injectors will provide flexibility in phasing that could enable plasma current profile control by varying the fluctuation profile required for IDCD, and also lead to bulk plasma rotation when the injectors are phased appropriately.

3.4. Pumping requirements

In any DT fusion reactor, helium ash must be promptly removed from the plasma via some method of pumping to avoid plasma dilution and maintain steady-state operation. The total fusion power of the dynomak operating point is 1953 MW, which equates to a helium production rate of approximately 6.9×10^{20} s^{-1}. It is desired to keep the helium concentration of the plasma at or below 3% due to dilution concerns. The pumping requirements for the dynomak reactor concept is highly dependent on the edge density. Using the Grad–Shafranov pressure profile, the normalized separatrix pressure is expected to be 0.15%, which equates to a pressure of roughly 6640 Pa while assuming a 200 eV separatrix temperature that is consistent with the Ohmic power calculation discussed previously.

Assuming a magnetically insulated, wall-supported pressure from the separatrix to the wall, and a 10 eV temperature at the wall to limit sputtering, the expected edge density is approximately 2.1×10^{21} m^{-3}. Using the conductances of the pumping ducts, and the expected edge density and temperature, the dynomak is estimated to require a pumping capacity of 14.5 m^{3}s^{-1}. However, this estimation is a significantly lower pumping requirement than ITER, which is designed to have a thermal power of only 500 MW. As a more conservative estimate for the dynomak pumping requirement, the ITER pumping requirement is scaled linearly with the thermal power, which would yield 163 m^3 s^{-1} for 1953 MW [13]. Thus, there is a considerable range of possible pumping requirements that is highly dependent on the edge density, which is not known confidently for the dynomak concept; more substantive estimations of the edge density are a subject of future work. As a result, the pumping system is conservatively sized to allow for ITER-scaled pumping requirements if necessary, though it may be overengineered if the edge densities are as high as calculated using the constant, wall-supported pressure assumption between the separatrix and wall.

The dynomak pumping system is composed of a series of ducts connecting the main vacuum chamber to twelve cryosorption pumps connected in a toroidally continuous pumping manifold, as shown in Fig. 1. Exhaust gases will be pumped through 24 blanket penetrating ducts evenly spaced around the top and bottom of the

Please cite this article in press as: D.A. Sutherland, et al., The dynomak: An advanced spheromak reactor concept with imposed-dynamo current drive and next-generation nuclear power technologies, Fusion Eng. Des. (2014), http://dx.doi.org/10.1016/j.fusengdes.2014.03.072

inner confinement volume, as shown in Fig. 1. The ducts must be cooled due to the presence of fast-neutrons and residual plasma, which is achieved by linking to the first wall cooling system that will be described. The exhaust gases expand in the pumping manifold where they are removed by the connected, ITER-developed cryopumps.

3.5. Q_p and Q_e calculations

The plasma and engineering gain are typical figures of merit for plasma and reactor system performance. The plasma gain Q_p is defined by Eq. (8), where the fusion power P_{fus} is $P_\alpha + P_n$ and P_{CD} is the coupled current drive power to the plasma. This quantity can be thought of as a measure of the degree of self-sustainment (i.e. $Q_p \rightarrow \infty$ indicates ignition) or alternatively, the degree of control over the power balance of the system. Using the fusion power value of 1953 MW and the coupled current drive power requirement of 58.5 MW listed in Table 1, we find a plasma gain Q_p,

$$Q_p \equiv \frac{P_{fus}}{P_{CD}} \approx 33 \tag{8}$$

which is directly competitive with a recently assessed spherical torus 1 GWe DEMO and outperforms a similarly scaled tokamak DEMO [2]. This plasma gain competitiveness with devices that require substantially lower plasma currents for operation is a testament to the high efficiency of IDCD should it scale to reactor-relevant plasmas as expected.

The engineering gain Q_e, which is more appropriate for determining overall reactor performance and thus is of importance to power companies, is provided in Eq. (9). The wall plug efficiency η_{plug} is assumed to be 80% since 70% has been achieved on HIT-SI helicity injection system without optimization; however, more precise wall plug efficiencies will be obtained for each subsystem in the dynomak reactor concept in future work. The resistive power dissipation in copper P_{Cu} results from the FLiBe-cooled copper coils embedded in the FLiBe blankets near the outboard midplane, as depicted in Fig. 1. The superconducting dissipation is nearly zero; however, a modest steady-state cooling requirement for the superconducting coil set was included in the overall balance of plant. Lastly, the thermal efficiency of this reactor is expected to be upwards of 47% due to the use of an advanced, supercritical CO_2 Brayton cycle to be discussed. The expected powers for the parameters presented in Eq. (9) provides a engineering gain of approximately 9.5. This large engineering gain is attractive for power companies, and outperforms all recently assessed 1 GWe reactor scenarios in [2].

$$Q_e \equiv \frac{\eta_{th}\eta_{plug}(P_{th} + P_{CD} + P_{Cu})}{P_{CD} + P_{SC} + P_{Cu} + P_{pump} + P_{cooling}} \approx 9.5 \tag{9}$$

4. Blanket system

4.1. Choice of blanket material

A main motivator for the choice of blanket materials was to achieve a tritium breeding ratio (TBR) of greater than 1.1 without complex nuclear engineering. It was found from Monte Carlo N-Particle (MCNP5) neutron transport simulations that the TBR is highly sensitive to the first wall thickness, and thus it was advantageous to minimize the thickness of high-Z, non-tritium-breeding material between the fusion neutron source and the tritium breeding material. A unified, liquid blanket system was decided upon since it is optimal for obtaining a high TBR, and it realizes the engineering simplicity of using a single working fluid for first wall cooling, neutron moderation and tritium breeding.

The molten salt eutectic composed of BeF_2 and LiF, commonly referred to as FLiBe, was chosen as the working fluid due to its excellent moderation characteristics, sufficient tritium breeding capability, and its low electrical conductivity that reduces magnetohydrodynamic flow concerns [14,15]. Additionally, the ability to enrich FLiBe with Li-6 to increase the TBR is attractive due to uncertainties in the calculated TBR from MCNP5 simulations. If the experimental TBR is lower than expected from MCNP5 simulations, one can increase the concentration of Li-6 in the FLiBe to raise the TBR without physically changing the reactor unit. If the TBR is substantially lower than MCNP5 simulations and Li-6 enrichment does not suffice, an additional beryllium neutron multiplier can be placed on the outside of the primary vacuum vessel.

A corrosion concern that must be mentioned while considering FLiBe as the tritium breeding medium is the production of hydrofluoric acid. With ample free $^3H_2$ in the blanket, hydrofluoric acid is generated via Eq. (10),

$$2^3\,HF + M \leftrightarrow H_2 + MF_2 \tag{10}$$

where ^3H could be any other hydrogen isotope and M could be Fe, Cr, W, etc., depending on the surrounding structural materials, such as 316 SS in the dynomak blanket system [16]. Fortunately, the reduction of hydrofluoric acid in static FLiBe has been demonstrated by adding excess Be to utilize the redox reaction expressed in Eq. (11) [17].

$$2\,HF + Be \rightarrow H_2 + BeF_2 \tag{11}$$

Thus, it appears control of this corrosive agent that would likely be produced in a FLiBe blanket system is possible, and the introduction of addition Be to the system will also help to increase the TBR. Of course, confirmation of corrosion and erosion rates will be a necessity during the fusion nuclear science facility (FNSF) stage of a fusion development path, which will be discussed.

4.2. First wall and thermal hydraulics

The primary vacuum vessel as shown in Fig. 1 contains the DT plasma. Moving minor radially outwards, a thin alumina insulating layer is plasma-sprayed on a 1 cm thick, copper flux conserver. Maintaining this thin insulating coating may be accomplished by edge recycling. Vapor deposition of alumina occurs at 475–800 °C, with a maximum deposition rate at 500 °C [18,19]. Evaporation and sputtering will be faster at higher temperatures, and thus sputtering and redeposition may regulate the plasma facing surface to nearly a uniform temperature. With nearly uniform wall loading and cooling, the thickness of the alumina layer will be kept uniform. A negative density gradient in the plasma will tend to keep the sputtered and evaporated material out of the plasma, reducing impurity contamination. However, the oxygen and aluminum that is pumped out must be reintroduced into the system during steady-state operation, possibly via plasma spraying the first wall with the insulator material via low-level impurity injection. The surface temperatures of the vacuum ducts and the injectors can be controlled by varying coolant circulation rates in these areas to prevent loss or buildup of alumina on the surfaces. It is desired to conduct plasma-material interaction (PMI) tests of an insulating first wall coating with a large plasma heat flux before steady-state operation is attempted.

The copper flux conserver serves the main purpose of providing a highly electrically conducting shell that is beneficial for plasma stability. Any excursion from equilibrium will lead to a change in magnetic flux intersecting the walls that will induce stabilizing eddy currents. Thus, a highly conducting first wall close to the plasma boundary increases the passive stabilization capability of the system and decreases instability growth rates, enabling the

Please cite this article in press as: D.A. Sutherland, et al., The dynomak: An advanced spheromak reactor concept with imposed-dynamo current drive and next-generation nuclear power technologies, Fusion Eng. Des. (2014), http://dx.doi.org/10.1016/j.fusengdes.2014.03.072

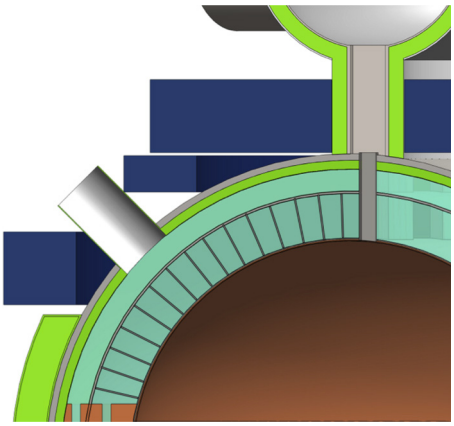

Fig. 8. The dual-chambered FLiBe blanket system with representative minor radial cooling pipes carrying relatively cool FLiBe from the 25 cm thick, pressurized outer blanket to the first wall cooling system. The first wall cooling system then exhausts to the 50 cm thick hot blanket, where is it neutronically heated to the reactor outlet temperature of 580 °C.

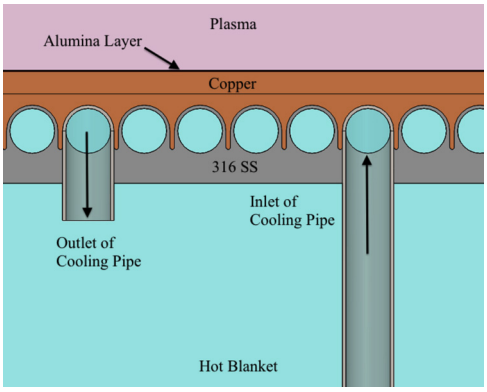

Fig. 9. The first wall cooling system. Note the FLiBe input pipe carries FLiBe at 480 °C to the first wall, where it will flow toroidally around in both directions for 4.3 m until exhausting to the hot blanket at 509 °C. This figure depicts a single cold pipe out of approximately 5700 pipes required to adequately cool the first wall. After exhausting to the hot blanket at 509 °C, the 50 cm hot blanket is heated to 580 °C via neutron moderation and exothermic lithium reactions, which is the global reactor outlet temperature.

plasma to be stabilized against resistive wall modes with a modest amount of intrinsic or injector imposed rotation. Additionally, copper is an excellent thermal conductor, which is favorable for coupling the FLiBe cooling system to the plasma facing first wall to remove the plasma heat effectively.

A series of 316 SS FLiBe cooling tubes are bonded to the copper first wall to ensure good thermal contact. These first wall cooling tubes are linked to a dual-chambered, pressurized FLiBe blanket system as shown in Fig. 8. The upward of 5700 minor radial cooling pipes take FLiBe at 480 °C from the 25 cm thick, cold blanket and transport it to the first wall cooling tubes, which have an internal diameter of 1.2 cm and a toroidal length of 4.3 m. The FLiBe flows through these cooling tubes at 8 ms^{-1}, which then is exhausted to the hot blanket at 509 °C. The majority of the fusion neutrons moderate in the 50 cm hot blanket and hence this is where the majority of tritium is generated as well. With a chosen global volumetric flow rate of FLiBe of 5.17 $m^3 s^{-1}$, the outlet temperature of the hot blanket before coupling to the secondary, supercritical CO_2 Brayton cycle is 580 °C.

The FLiBe cooling tubes that are integrated as part of the primary vacuum vessel are welded to a 1 cm thick, 316 SS surface for structural support, which interfaces with the 50 cm hot blanket. A 2 cm thick, 316 SS structural shell separates the hot from the cold blanket, the latter of which is pressurized to 0.86 MPa. The first wall cooling pipes in the hot blanket provide the structural support for the first wall module, whereas the 2 cm thick 316 SS separator is connected to the outer, 316 SS reactor shell via a truss system (not depicted in Fig. 1) in the 25 cm cold blanket that allows for poloidal FLiBe flow. The truss system connects to another 2 cm thick, 316 SS shell, 10.5 cm of ZrH_2 for neutron shielding, and then the primary 7.5 cm stainless structural shell that will serve as the final pressure vessel boundary before the biological containment structure. Additional neutron shielding is placed along the outboard midplane of the reactor to protect the superconducting pull coil from fast neutrons passing through the helicity injector region. A characteristic slice of the first wall cooling system in depicted Fig. 9.

The velocity of the FLiBe and toroidal length of cooling pipes were chosen to prevent the non-structural copper flux conserver from becoming structurally unsound under its own weight due to its high operating temperature relative to its melting point. Additionally, it is desired to keep the 316 SS reasonably cool in an effort to maintain a high yield strength for possible disruption events. A maximum temperature for the alumina surface was chosen to be 670 °C, while the temperature difference between cold input and hot output of the FLiBe cooling tubes was chosen to be 29 °C, starting from a base cold blanket temperature of 480 °C. The Dittus–Boelter equation for the Nusselt number of a turbulently flowing, non-metallic fluid in a round heated pipe was used to derive an expression for the required velocity to obtain a particular convective heat transfer coefficient h. Given a hydraulic diameter of 12 mm, a flow velocity of 8 ms^{-1} is required with a 4.3 m long, toroidally running pipe subject to the plasma heat flux through the copper interface. This velocity is required for all 5700 tubes within the stainless shell in order to keep the first wall adequately cool. Future research will include studying the behavior of FLiBe at high (greater than 1 ms^{-1}) speeds, with special attention paid to erosion rates and localized cavitation [17]. The choice of materials for the first wall and blanket assemblies yields a requirement for shallow burial or storage of low level radioactive waste for 100 years prior to being handled by hand for recycling purposes, assuming a power loading of 4.2 MW m^{-2} for 25 years [20]. Recycling before 100 years of storage could be possible through robotic means. Overall, a required storage period of 100 years is deemed acceptable and is still a considerable benefit over typical waste storage requirements for fission reactors. Different choices of first wall materials, namely, the use of a different highly conducting material for a flux conserver may reduce material activation to nearly negligible levels. Additionally, the use of copper in a DT neutron environment is speculative, thus additional research is required to determine the maximum allowable displacements per atom for this first wall component. Advanced, dispersion strengthened copper may prove to be less susceptible to void swelling, which is the main concern at the desired temperatures of operation (≈600 °C) [34]. However, these alloys must be tested in the FNSF phase of the development path to be described later. In assuming dispersion strengthened copper may prove to be an acceptable material in a DT neutron environment, copper is one of the most established and currently manufacturable materials that has excellent electrical conductivity required for a plasma stabilization, and also serves as a neutron multiplier that enables a sufficient TBR with a FLiBe blanket without Li-6 enrichment.

4.3. Tritium breeding

A blanket system must be capable of achieving a TBR of greater than 1 for a closed DT fuel cycle, while a TBR > 1.1 is preferred due to losses during the tritium extraction process and uncertainties in tritium breeding simulations. The TBR was calculated using a

Please cite this article in press as: D.A. Sutherland, et al., The dynomak: An advanced spheromak reactor concept with imposed-dynamo current drive and next-generation nuclear power technologies, Fusion Eng. Des. (2014), http://dx.doi.org/10.1016/j.fusengdes.2014.03.072

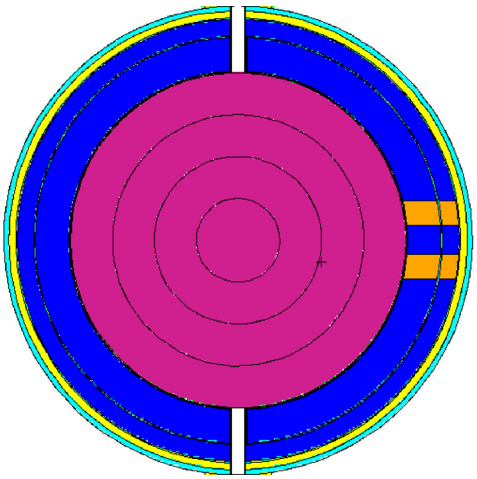

Fig. 10. A poloidal slice of the toroidal MCNP5 model used for TBR calculations. The pink region is the thermonuclear plasma with a weighted DT neutron source to accurately represent the expected neutron distribution from the pressure profile. Blue is FLiBe with natural lithium content with temperature dependent densities. Orange is the 35% FLiBe filled copper coils used for excluding flux from the injector region. Yellow is the ZrH_2 neutron shield surrounding the entire vacuum vessel. And cyan is 316 SS that forms the first wall cooling system material that couples to the copper first wall, the blanket separator, and the final pressure vessel of the entire system. Note the toroidally continuous vacuum pumping gaps that tend to overestimate the loss of neutrons from the system since the dynomak has discrete ducts that encompass only half of the toroidal circumference at their major radial location. (For interpretation of the references to color in this figure legend, the reader is referred to the web version of the article.)

Monte-Carlo N-Particle neutron transport code (MCNP5) with key reactor components that affect the TBR, namely, the first wall configuration and materials, the thicknesses of the FLiBe blankets, and the FLiBe-cooled copper coils used for excluding flux from the injector region of the reactor. A plot of the geometry used for the tritium breeding calculation is provided in Fig. 10.

The first wall was approximated to be poloidally continuous toroidal shells of appropriate thicknesses to accurately model the average thickness of FLiBe in the first wall cooling channels. A toroidally continuous vacuum gap was used as shown in Fig. 10 for the TBR calculation; however, this overestimates the loss of FLiBe resulting from the inclusion of pumping ducts since they only encompass approximately half of the toroidal circumference. In an effort to correct for this geometric inaccuracy, a simulation was run to determine the reduction in TBR solely from the vacuum ducts, and then this factor was corrected by 50% for the final TBR result. Additionally, the volumetric loss of FLiBe for the inductive helicity injectors was quantified, and was used to correct the TBR as well. With a FLiBe-cooled first wall, a 50 cm hot blanket of FLiBe, 25 cm cold blanket of FLiBe, 35% FLiBe filled copper coils for cooling and including the loss of FLiBe in the helicity injector region, a TBR of 1.125 ± 0.022 was calculated. The large quantity of copper in the first wall provides ample neutron multiplication, and most neutrons are thermalized within the first 50 cm of the FLiBe blankets. Quantitatively, nearly 85% of tritium production occurs in the 50 cm thick, hot FLiBe blanket. Also, the copper coils immersed in the FLiBe blankets nearly offset the negative effect of removing FLiBe blanket volume for the coils since they are partially filled with FLiBe and provide considerable neutron multiplication.

The only components not included in this MCNP5 analysis are the radial pipes in the hot blanket and the trusswork in the cold blanket. However, the FLiBe volume losses resulting from the inclusion of these components are estimated to be 1–2% of the total blanket volume, and so the total TBR should be maintained above 1.1. If future, refined simulations indicate the TBR has decreased below the desired minimum value of 1.1, Li-6 enrichment of FLiBe is a possible approach to increase the TBR, or adding a beryllium multiplier outside of the 316 SS first wall structural shell. In short, it appears a sufficient TBR for this reactor plausible since all avenues for maximizing tritium production have not yet been exploited.

4.4. Shielding

Though FLiBe is an excellent moderator, with a mean free path of 7 cm for 14 MeV fast neutrons [14], neutron shielding is required around the reactor system to protect the sensitive superconducting coil set from residual fast neutrons. Fast neutron (i.e. neutrons with energy greater than 0.1 MeV) damage to niobium-tin superconductors have been documented to reduce the critical current density at neutron fluences of 3×10^{22} m^{-2}. A coil can quench if the superconducting strands do not operate below the critical current density throughout the coil lifetime [5]. Since YBCO superconductor is expected to exhibit critical current density degradation at some value of fast neutron fluence yet to be determined, shielding of fast neutrons is of importance for the dynomak equilibrium coil set. Generally, materials with high mass fractions of hydrogen are desired from elastic scattering considerations since they enable a thin neutron shield to be used, which can reduce cost. However, neutron shielding is more complex than simple elastic scattering considerations, and a composition of high-Z atoms in the shielding material is also effective at attenuating fast neutrons [21]. Another consideration is that the proximity of the superconducting coils to the equilibrium sets the required currents to achieve force balance or assist in excluding flux from the injector region. As superconducting coils move further away from the plasma equilibrium, the required coil currents rise to provide the necessary push or pull on the equilibrium. In particular, the pull coil on the outboard midplane working in concert with the two FLiBe-cooled copper coils to exclude flux from the injector region was found to be of greatest concern in this concept. Thus, advanced, thin neutron shields that protect superconductors sufficiently are desired from the standpoint of safer operation of superconducting coils, that is, in a regime far from the critical current densities or $j \times B$ stress limits.

It is known that the inductive helicity injectors introduce a limiting 14.1 MeV neutron beam that passes through the injector mouth with negligible interaction with moderating FLiBe. As a result, an additional neutron shielding module was introduced on the midplane of the reactor, as depicted in Fig. 1. Two neutron shielding materials were considered for the dynomak reactor system, ZrH_2 and $Zr(BH_4)_4$, which both have the favorable shielding attributes of high hydrogen mass fractions and high-Z nuclei. The attenuation of 14 MeV fast neutrons versus thickness of various materials of interest is presented in Fig. 11 [21]. It is clear for a thickness of 50 cm, ZrH_2 attenuates fast neutrons far more effectively than $Zr(BH_4)_4$, and thus was the material of choice for the neutron shielding module. An attenuation coefficient of 2.9×10^{-5} was derived from Fig. 11 while considering the neutron power loading provided in [21]. Using the neutron wall loading from Table 1, and an estimation for the YBCO neutron fluence degradation threshold of 5×10^{18} cm^{-2} motivated by [5], a 50 cm ZrH_2 shield enables a pull coil lifetime of 29.3 full-power-years (FPY). Also, 25 cm of neutron shielding was placed on either side of the pumping ducts as shown in Fig. 1. An MCNP calculation confirmed the fast neutron flux on the coils next to the pumping ducts was sufficiently low, such that the limiting coil lifetime of all superconducting coils used in this concept is the outboard midplane pull coil at 29.3 FPY.

4.5. Choice of secondary cycle

In an effort to maximize the overall efficiency of the reactor concept in generating electricity, and enable operation in the desired temperature range of 480–580 °C, both helium and

Please cite this article in press as: D.A. Sutherland, et al., The dynomak: An advanced spheromak reactor concept with imposed-dynamo current drive and next-generation nuclear power technologies, Fusion Eng. Des. (2014), http://dx.doi.org/10.1016/j.fusengdes.2014.03.072

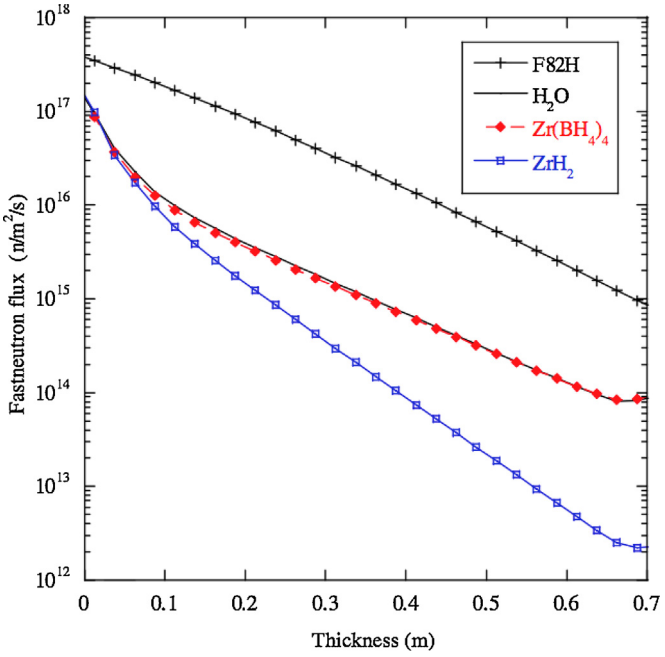

Fig. 11. ZrH_2 and $Zr(BH_4)_4$ neutron shielding versus shield thickness [21], compared to pure water and F82H steel. Note the superior fast neutron attenuating capabilities of ZrH_2 for a shield thickness of 50 cm that will be used for the outboard midplane shielding module. For the thinner, 10.5 cm neutron shield around the entire reactor assembly as shown in yellow in Fig. 10, ZrH_2 was still determined to be the most effective material, however, not by as large of a margin as with the 50 cm outboard midplane shield.

supercritical CO_2 Brayton cycles were considered for the secondary, power conversion cycle. A supercritical CO_2 power cycle was ultimately chosen due to the compact size of the system that reduces the power plant footprint, and also due to the attractive thermal efficiency expected to be at least 45% within the desired range of operating temperatures [22,23]. The viability of a supercritical CO_2 secondary cycle has been reviewed favorably by Westinghouse Electric Company for next-generation, molten salt fission plants, suggesting this nuclear power technology is a reasonable choice for this reactor concept [24]. Due to the relatively conservative range of operating temperatures, material degradation concerns and complex heat exchanger designs common to very high temperature reactors [25] (i.e. temperatures $\geq$900 °C) will likely not be required. Even so, detailed design of heat exchanger units for coupling the FLiBe primary loop with the supercritical CO_2 secondary cycle should be completed in future work.

5. Economics

One of the major, unresolved issues preventing the widespread adoption of fusion energy is not technological, but rather economic in nature. For fusion to be considered an economically viable energy source to displace fossil fuels, such as coal and natural gas, it is imperative for fusion to provide electricity for a price that power companies, and ultimately consumers, are willing to pay. The benefits of fusion energy are very motivating: zero greenhouse gas emissions, no long-lived radioactive waste and a nearly unlimited fuel supply. These benefits may justify slightly higher costs of electricity when compared to conventional power sources. However, practically speaking, fusion must provide economical electricity to have a large impact on the energy industry in the United States during this century.

As has been mentioned previously, toroidally linked devices such as tokamaks and stellarators that rely on superconducting coils to provide some or all of the magnetic fields for confinement and stability suffer from two fundamental issues that become more pronounced as the system becomes more compact: fast neutron fluences and $j \times B$ stresses on the inboard section of the superconducting coils encircling the vacuum vessels. Due to the relatively low-β plasmas characteristic of tokamak and stellarator configurations, it is typical to use high-fields to exploit the quartic dependence of the fusion power density on magnetic field. However, in compact configurations with high fields, very large $j \times B$ structural stresses are created that require aggressive engineering and use of robust superstructures to withstand the electromagnetic forces. Additionally, one must consider the nuclear engineering complexity required to achieve a sufficient TBR in a compact configuration. As a larger fractional blanket volume for neutron shielding of the inboard superconducting coils is required, the TBR decreases precipitously. However, this shielding is necessary to ensure an economical lifetime of these expensive components.

Thus, in short, it is difficult to make compact, reactor scale tokamaks and stellarators with high fusion power densities to achieve competitive costs of electricity, because of the requirement of toroidally linking superconducting coils in various forms. Instead, the dynomak concept, based on the spheromak configuration, enjoys more efficient plasma confinement with a wall averaged β of 16%, and the elimination of a toroidally linking superconducting coil set. These features enable a more compact reactor system overall by eliminating the aforementioned neutron fluence and $j \times B$ limitations. The dynomak reactor concept will be argued to be more economically attractive than other fusion reactor concepts, and suggested to be competitive with conventional fossil fuel sources.

5.1. Economic requirements

The overnight capital costs for various energy sources provide a metric of comparison to assess the economic viability of fusion energy. It should be noted that overnight capital costs do not include interest payments on borrowed capital, nor does it include maintenance costs; however, these costs will be assessed in future work. According to the U.S. Energy Information Administration's recent analysis of overnight capital costs for various types of power plants, the cheapest energy source for the generation of electricity is natural gas [26]. Natural gas has the lowest overnight capital cost per kW by a considerable margin, with an expected $665 per kW for an advanced compact turbine (CT) [26]. Adding carbon capture technologies to a CT or using other methods of natural gas electricity generation provides a range of overnight capital costs from $974 - $2060 per kW [26]. The closest traditional competitor, coal, has a lowest overnight capital cost of $2844 per kW. It is suggested that a competitive fusion reactor overnight capital cost, disregarding the benefits of zero greenhouse gas emissions that may justify slightly higher costs, is in the range of $665–2844 per kW. Granted, future carbon taxes on emissions may further improve the case for fusion energy when compared to fossil fuels; however, no such taxes are assumed in this study to improve the economic viability of the dynomak reactor concept.

5.2. Dynomak costing

As with the pricing of any conceptual fusion power plant, the price of many components are difficult to determine since large scale means of production have not yet been established. Assumptions concerning the price reductions of components for a *n*th-of-a-kind fusion reactor due to advanced manufacturing techniques are usually integrated into the price estimates of proposed commercial plants that help provide attractive costs of electricity (COE) [4,27]. More specifically, the high-temperature

Please cite this article in press as: D.A. Sutherland, et al., The dynomak: An advanced spheromak reactor concept with imposed-dynamo current drive and next-generation nuclear power technologies, Fusion Eng. Des. (2014), http://dx.doi.org/10.1016/j.fusengdes.2014.03.072

Table 4
Dynomak reactor concept cost breakdown. The asterisks denote components of the cost analysis that were taken from the ARIES-AT study [4] and inflation corrected to 2013 dollars.

Component(s)	Cost ($M)
Land and land rights*	17.7
Structures and site facilities*	424.3
Reactor structural supports	45.0
First wall and blanket	60.0
ZrH_2 neutron shielding	267.4
IDCD and feedback systems	38.0
Copper flux exclusion coils	38.5
Pumping and fueling systems	91.7
Tritium processing plant	154.0
Biological containment	50.0
Superconducting coil system	216.0
Supercritical CO_2 cycle§	293.0
Unit direct cost	**1696**
Construction services and equipment*	288
Home office engineering and services*	132
Field office engineering and services*	132
Owner's cost*	465
Unit overnight capital cost	**2713**

superconductors implemented in this concept are largely uncharted economic territory and assumptions concerning the price of these expensive components must be estimated in some manner. Since the cost reductions for large-scale manufactured YBCO superconductors are uncertain due to the infancy of production process, reducing the quantity of superconductors to a single, non-interlinking, circular coil set with a modest peak field on coil of 6.5 T will likely result in a substantially cheaper reactor when compared to a tokamak or stellerator with a similar thermal power.

In an effort to estimate the cost of the dynomak reactor system as substantively as possible, ITER pricing will be used for many components and scaled as seen appropriate, such as the fueling, vacuum, and tritium separation and processing plant systems. High-temperature superconducting coil set figures will be presented conservatively based on recent cost figures for second generation YBCO wire of recent interest to the U.S. DOE [28]. A pricing metric based on previous projects by Westinghouse Electric Company for bulk material costs of fission plants is to use the raw material costs and multiplying by two, and then adding the estimated manpower contribution to the price of reactor components [24]. In this study, the bulk material costs of large reactor components, such as the nearly toroidal copper and stainless steel shells of the reactor unit, will be two times the cost of high quality sheets of these materials at relevant thicknesses. Additionally, for the piping system that cools the first wall and connects the outer FLiBe blanket manifold to the first wall system, two times the stainless steel piping cost will be used as an estimation for the cost. A conservative estimate for the cost of FLiBe of $75 per kg was chosen from the range provided by the APEX group [15], along with estimates for a supercritical CO_2 secondary power conversion cycle from a recent study concerning the use of this advanced Brayton cycle on next-generation fission reactors [22]. Lastly, a cost estimation for the biological containment structure was included, as well as the expected cost for ZrH_2 neutron shielding.

The overnight capital cost analysis of the dynomak reactor concept is presented in Table 4 with relevant subsystems that contribute significantly to the overall cost. The components listed with asterisks denote inflation corrected figures from the ARIES-AT study [4] that were deemed applicable to the dynomak reactor concept. Of special note, the high-temperature superconducting coil set for the dynomak was priced using a production cost of \$36 kA m^{-1} that is argued to be reasonable using HTS wire being developed at American Superconducting Corporation [28] as a cost basis. This costing assumption results in a superconductor coil set for the dynomak that is approximately the same price as the ARIES-AT magnet system after being adjusted for inflation, despite having two less coil sets than ARIES-AT. Thus, we deem the superconducting coil set pricing conservative when compared to the ARIES-AT study. It should also be noted that as Li-6 in FLiBe is degraded over time, more FLiBe must be added to ensure a sufficient TBR is maintained, though this cost will be treated as a fuel cost and is estimated to be quite reasonable over the lifetime of the plant. With these stated assumptions and metrics for costing, the dynomak reactor system cost analysis results in a unit direct cost of $1696 per kWe and a overnight capital cost of $2713 per kWe in 2013 USD.

From this economic analysis, it is suggested the dynomak reactor concept may provide an economical path towards fusion power, provided the speculative IDCD mechanism scales to reactor-relevant plasmas as expected and is compatible with good energy confinement. Clearly, substantial research and development is required prior to constructing a spheromak reactor based on IDCD, and these requirements will be described in detail. However, provided IDCD scales as desired, by eliminating the toroidal field coils and utilizing this energy efficient current drive mechanism, a compact, cost effective fusion reactor may be plausible. It should be noted that with the cost estimates provided in Table 4, the dynomak reactor concept overnight capital cost is within the previously suggested range of $665 - $2844 per kW to be competitive with conventional power sources. If these cost estimates are indeed conservative, then the dynomak reactor concept may be able to be built more cheaply, and thus become more competitive with natural gas [26].

Lastly, it is recognized that overnight capital cost is not the only economic consideration for a viable power plant; it is imperative to address the maintenance costs over the power plant lifetime to assess its overall economic viability. Detailed maintenance costs and procedures are a subject of future work; however, it should be noted that the most expensive components of the dynomak reactor concept, namely the neutron shielding, superconductors, and FLiBe, are essentially lifetime components and thus are nearly completely accounted for (apart from the additional FLiBe required to maintain a natural Li-6 concentration) in the overnight capital cost. The first wall assemblies will require replacement during regular maintenance periods due to various forms of material damage expected in a DT fusion environment, which will be better assessed in the fusion nuclear science facility (FNSF) stage of development path to be described. However, the overall cost of the first wall assembly is a small fraction of the overnight capital cost, and may be offset by the substantially lower annual fuel costs when compared to fossil fuels.

6. Key research requirements and future work

The conceptual analysis of the dynomak reactor system has uncovered a multitude of research requirements. The most important research requirement is the demonstration of IDCD-enabled profile control on the HIT-SI3 experiment that is beginning operations at the University of Washington [29]. The previous HIT-SI device had two helicity injectors placed on either side of the machine, phased by 90° to enable a constant rate of helicity injection [1]. The new HIT-SI3 device has three helicity injectors located on a single side of the confinement volume, and with flexibility of injector phasings, could enable plasma current profile control by changing the imposed fluctuation profile that is responsible for IDCD.

Provided plasma current profile control is demonstrated in HIT-SI3, the key risk reduction experiment on the path towards

Please cite this article in press as: D.A. Sutherland, et al., The dynomak: An advanced spheromak reactor concept with imposed-dynamo current drive and next-generation nuclear power technologies, Fusion Eng. Des. (2014), http://dx.doi.org/10.1016/j.fusengdes.2014.03.072

a spheromak reactor system enabled by IDCD is a PoP experiment. The main purpose of this experiment is to demonstrate that adequate energy confinement is compatible with the magnetic fluctuations required for IDCD. Recent simulations have suggested the conventional view that magnetic fluctuations are responsible for severe confinement degradation is not correct. Instead, the correct causal relationship appears to be that instability causes confinement degradation, and magnetic fluctuations accompany instability, but the fluctuations themselves do not severely degrade confinement. This conclusion is substantiated by NIMROD simulations of a larger HIT-SI device that suggest the existence of closed flux over many injector cycles with an imposed magnetic fluctuation amplitude of $\delta B/B \approx 10^{-1}$, whereas closed flux was destroyed if the equilibrium went unstable. In a reactor, the magnetic fluctuation amplitude will be considerably smaller ($\approx 10^{-5}$) due to higher current gains, which should further reduce the deleterious effects of magnetic fluctuations on energy confinement to manageable levels. Additionally, demonstration of reasonable IDCD power requirements by obtaining the desired temperature profile is necessary for the advancement of this concept. The HIT-PoP experiment size and operating point will be described in the next section.

As with any fusion reactor, a fusion nuclear science facility (FNSF) will be required to experimentally assess first wall damage, tritium breeding self-sufficiency, material activation, adequate superconductor shielding, and the overall structural integrity of all materials in a DT fusion environment. A pedigree of material performance in a DT neutron environment must be established during the FNSF phase before proceeding to commercialization. It should be noted that 316 SS and copper were the main materials of choice for the first wall of the dynomak concept. The copper flux conserver, which is not a structural component, is bonded to the 316 SS cooling tubes, which are then welded to the 316 SS structural shell to complete the primary vacuum vessel. It is intended to have a rapid maintenance cycle of the modular, first wall assembly such that the 316 SS components do not exceed 20 displacements per atom (dpa). More advanced, ferritic/martenistic steels rated for the desired temperature range of operation may be used in the future that could enable a longer first wall lifetime [33]. Additionally, as was mentioned before, more advanced, dispersion strengthened copper may reduce void swelling concerns and enable a reasonable first wall replacement frequency [34]. However, for the sake of substantive pricing and using established, well known materials for this concept, the choice of 316 SS and copper is maintained. Final material choices for commercialization will be made following results from the FNSF phase of the development path.

The choice of high-temperature superconductors in the dynomak reactor concept introduces the research requirement of establishing large scale manufacturing and winding of high temperature superconducting coils that is presently not available, and was assumed to be accomplished by advanced manufacturing methods in the ARIES-AT study [4]. YBCO superconductors have substantially higher costs than niobium based superconductors [31] due to this lack of well established, cost effective, large-scale manufacturing [28]. YBCO was chosen for this reactor system primarily due to the ease of using subcooled liquid nitrogen instead of liquid helium required by niobium-based superconducting strands, and the possible smaller amount of quench material required for YBCO [31] that may enable smaller coils on a total mass basis. Even with these benefits, if price reductions do not occur as expected for YBCO superconductors, since the peak field on coil is only 6.5 T in the dynomak reactor system, utilizing more established niobium based superconductors is feasible. This choice of superconducting material would reduce the cost of the superconducting coil set in the short term. Thus, due to the relatively low peak magnetic field on coil in the dynomak reactor concept, there is considerable flexibility in the choice of superconducting material.

Detailed heat exchanger design for coupling the FLiBe primary loop with a supercritical CO_2 secondary cycle must be carried out and experimentally tested at the desired temperature range of operation. Since the peak temperature of the reactor system is 580 °C, aggressive heat exchanger designs and use of exclusively high-temperature materials that is characteristic of very high temperature fission reactors (i.e. temperatures of ≥900 °C) [25] will likely not be required for this reactor concept, and should enable a reasonably priced solution. Nevertheless, the design should be completed with future work to ensure such a cost effective solution is feasible.

As has been the subject of recent work, power exhaust characteristics and the coupling of the injector fields to the equilibrium must be studied on both the HIT-SI3 and HIT-PoP experiments. The magnetic topology of the last closed flux surface and scrape of layer (SOL) in the dynomak reactor will be dynamic due to the oscillatory nature of the injector fields. The desired operating point is a magnetically insulated, wall supported plasma that provides a large edge density for ease of pumping and also enables operation in a detached plasma state while maintaining a 200 eV separatrix required for attractive IDCD power requirements. An optimization must be conducted with more detailed experimental and simulation analyses concerning injector power coupling to the equilibrium with a cool, resistive edge required for power removal, reasonable pumping requirements, and low sputtering yields.

7. Development path

7.1. HIT-SI3

The HIT-SI3 experiment, shown in Fig. 7, is constructed and will be operational by April 2014. The use of three injectors allows flexibility in the types of phasing that result in a time averaged injection of helicity required for sustainment (i.e. in-phase or each injector 120° out-of-phase like a three-phase motor). By varying the phasing of the injectors, HIT-SI3 may demonstrate plasma current profile control via changing the imposed magnetic fluctuation profile that is responsible for current drive.

As was discussed previously, profile control is critical for the advancement of the dynomak concept since it would enable controlled operation of a stable magnetic equilibrium. Additionally, with each injector operating 120° out-of-phase with one another, one can impose a torque that should result in bulk plasma rotation. Thus, HIT-SI3 may demonstrate driven plasma rotation with appropriate injector phasings, which is known to be beneficial for overall plasma stability and the suppression of resistive wall modes [32]. Additionally, use of new edge probes and two-photon laser induced fluorescence will provide neutral density information about energy transfer in the system, and, more specifically, how injected power from the helicity injectors couples to the spheromak equilibrium. This information, together with neutral density dynamics in simulations of HIT-SI3 that include the non-axisymmetric injectors, will provide more predicative models for energy transfer and power coupling of the injectors to the equilibrium.

7.2. Proof of principle experiment (HIT-PoP)

Provided profile control is demonstrated on HIT-SI3, the PoP experiment will be the main risk reduction experiment that will addresses the viability of IDCD as a sustainment mechanism for controlled fusion energy. As was described before, there is computational evidence that suggests magnetic fluctuations may be compatible with good confinement. HIT-PoP is chosen to have a

Please cite this article in press as: D.A. Sutherland, et al., The dynomak: An advanced spheromak reactor concept with imposed-dynamo current drive and next-generation nuclear power technologies, Fusion Eng. Des. (2014), http://dx.doi.org/10.1016/j.fusengdes.2014.03.072

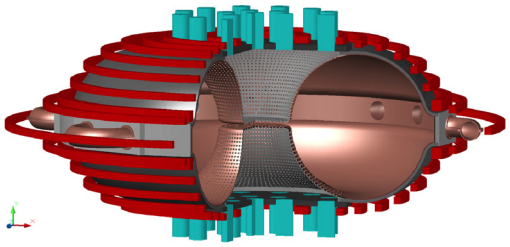

Fig. 12. The HIT-PoP experiment with a major radius of 1.5 m and minor radius of 1.0 m. The experiment is pulsed over 10 s and has a copper coil set in an effort to reduce cost when compared to superconductors. The total plasma current is 3.2 MA with a volume-averaged number density of 5×10^{19} m^{-3}. The center column is perforated to allow for pumping with the cyan colored cryopumps located on both the top and bottom of the machine. IDCD helicity injectors are located on the outboard midplane like the dynomak reactor system, and will serve as the first experimental test of the injectors in this type of configuration. A 1 cm thick copper flux conserver coupled with a strongly sheared q-profile enables stable, high-β operation. (For interpretation of the references to color in this figure legend, the reader is referred to the web version of the article.)

major radius R_o of 1.5 m and a minor radius a of 1.0 m, which is deemed an appropriate size to have an adequate safety margin for all plasma and engineering parameters of interest. The toroidal plasma current is 3.2 MA with a volume-averaged electron number density of 5×10^{19} m^{-3}. Thus, the HIT-PoP experiment is sized to allow for acceptable plasma performance and will have a substantially lower fluctuation amplitude ratio due to higher current gain, which should allow for reactor relevant energy confinement to develop during a ten second pulse. HIT-PoP will answer the key question of whether IDCD is a viable approach to the sustainment of a spheromak equilibrium, gauged by providing plasma current profile control with a reasonable current drive power requirement while maintaining sufficient energy confinement throughout the plasma current flattop.

The proposed HIT-PoP experiment is depicted in Fig. 12, including the copper coil set in red, cyan colored cryopumps, perforated center flux conserver that enables density control, and outboard, midplane IDCD helicity injectors. This is a pulsed machine, and the total power loading on the first wall will decrease from the HIT-SI experiment. This reduction in power loading is due to the the scaling of the IDCD power requirements with minor radius [1] versus first wall surface area increase. With an appropriately chosen pulse length of 10 s, it was determined a first wall cooling system is not required for this stage of the development path. HIT-PoP is a solely deuterium experiment and will have a peak on-magnetic-axis temperature of 3 keV. Provided the HIT-PoP experiment yields the desired results, the next stage involves an upgrade of the PoP experiment into the performance extension (PX) experiment.

7.3. Performance extension experiment (HIT-PX)

The HIT-PX experiment is an upgrade of the HIT-PoP experiment in that it is an identically sized machine (R_o = 1.5 m, a = 1.0 m) that is outfitted for steady-state operation and with blanket assemblies. The copper coil set is replaced by a superconducting coil set to enable energy efficient, steady-state operation and also allows for the demonstration of a superconducting equilibrium coil set with feedback control that will be required for the commercial scale reactor system. The dual-chambered, pressurized blanket system is added in this phase of the development path. However, instead of using relatively expensive FLiBe as the working fluid, HIT-PX uses water cooling in an effort to reduce the cost of this upgrade. Lower temperature blanket operation with water will reduce material degradation concerns at this stage of the development cycle, and will enable the demonstration of steady-state deuterium operation of a high performance spheromak configuration sustained with IDCD. Additionally, this choice of working fluid will provide FLiBe-relevant information concerning the thermal hydraulics of the blanket system, which could necessitate modifications before the addition of FLiBe and the corresponding increase in blanket temperatures. The peak, on-magnetic-axis temperature of this experiment will be upwards of 6–8 keV; however, with solely deuterium operation, water cooling should be sufficient for steady-state, high performance plasma operation. Provided the desired results are produced with HIT-PX, a fusion nuclear science facility (FNSF) is constructed via an upgrade of the PX experiment.

7.4. Fusion nuclear science facility (HIT-FNSF)

As with any fusion reactor development path, to address the lack of material degradation data in a DT fusion environment, a fusion nuclear science facility is required. The HIT-FNSF will be another upgrade of the HIT-PX experiment, which will include the replacement of water in the blanket system with FLiBe, and a corresponding increase in blanket operation temperature. The introduction of FLiBe at this stage, and the introduction of tritium for DT plasma operation, will provide the reactor relevant nuclear environment for testing of materials in the first wall and blanket system, and the high heat fluxes required to test the first wall cooling system. Additionally, the FNSF will allow for the demonstration of tritium breeding self-sufficiency. With a peak on-magnetic-axis temperature of 10–12 keV, the DT neutron yield will be considerable and thus ZrH_2 neutron shielding will be implemented in this phase of the development path to protect the superconducting, equilibrium coil set and reduce stray neutron fluxes to surrounding structural components.

The FNSF phase will provide valuable data on material degradation in a DT fusion environment, along with plasma-material interaction information. Additionally, a test of the tritium extraction efficiency from FLiBe and the tritium processing system will be demonstrated at this stage of the development path. Provided the desired results are produced in HIT-FNSF, and the appropriate engineering changes are made from what is learned from the FNSF stage of the development path, a pilot plant/demonstration spheromak reactor sustained by IDCD is built via an upgrade and/or rebuild of the FNSF experiment and performance ramp to reactor plasma parameters.

7.5. Pilot plant/DEMO reactor (HIT-DEMO)

The HIT-DEMO experiment is the critical stage for producing electricity from a spheromak configuration sustained by IDCD. Experimental parameters are ramped to power plant levels with a peak on-magnetic-axis temperature of 20 keV. As was stated previously, the HIT-DEMO reactor is the same size as HIT-PoP, HIT-PX and HIT-FNSF, with R_o = 1.5 m and a = 1.0 m. HIT-DEMO should provide net electricity once the high thermal efficiency, supercritical CO_2 power conversion cycle is coupled to the FLiBe primary loop that was simply exhausting heat to the environment prior to this stage of the development path. Though the small size of this pilot plant will likely not produce more than 20 MW electric, the demonstration of production of electricity from fusion energy is a necessity prior to commercialization. This size of experiment will provide the most cost effective means to achieve this goal. Then, it can be scaled to reactor relevant power outputs via an increase in size to the dynomak concept scale.

8. Summary

A conceptual, high-β spheromak reactor concept called the dynomak has been formulated around the newly discovered

Please cite this article in press as: D.A. Sutherland, et al., The dynomak: An advanced spheromak reactor concept with imposed-dynamo current drive and next-generation nuclear power technologies, Fusion Eng. Des. (2014), http://dx.doi.org/10.1016/j.fusengdes.2014.03.072

imposed-dynamo current drive (IDCD) mechanism. A guiding philosophy behind the dynomak concept is to utilize currently available materials and nuclear power technologies presently under development for next-generation fission power plants in an effort to accelerate development. Six, inductive helicity injectors located on the outboard midplane of the nearly doubly connected vacuum vessel are used to sustain a spheromak equilibrium with a toroidal plasma current of 41.7 MA. These six injectors with appropriate phasings may enable plasma current profile control from optimizing the imposed magnetic fluctuation profile. A simple, unified molten salt (FLiBe) blanket system is chosen for first wall cooling, neutron moderation and tritium breeding with no requirement for a divertor. A supercritical CO_2 Brayton cycle is used for the secondary power conversion cycle due to the compact size of components that reduces the physical footprint of the plant, and also due to the high thermal efficiency at the operating temperatures of interest (i.e. >45% with a peak reactor outlet temperature of 580 °C). Lastly, a high temperature, superconducting equilibrium coil set that is well protected by the FLiBe blanket and ZrH_2 neutron shielding is used with a limiting lifetime of at least thirty full-power-years. With these advancements, a reactor operating point with a thermal power of 2846 MW yields 1000 MWe with an IDCD power requirement of 73 MWe. The expected overnight capital cost of $2713 per kWe for the dynomak reactor concept is competitive with conventional power sources. Lastly, a thorough discussion of the research requirements, and a development path towards the dynomak fusion reactor is provided as a framework towards economical fusion energy using a spheromak configuration sustained by IDCD.

Acknowledgements

A special thank you to Zach Hartwig and the MIT PSFC ARC team for their assistance with getting started with MCNP and a convenient script for stacking MCNP card decks; it certainly saved a lot of time and was greatly appreciated. Also, thank you to Dr. Ed Lahoda of the Westinghouse Electric Company for providing insight into pricing reactor components and his support of a supercritical CO_2 secondary power cycle as a feasible next-generation nuclear power technology. Lastly, we are appreciative of Dr. Zinkle's input concerning the use of copper in a DT neutron environment.

References

[1] T. Jarboe, B.S. Victor, B.A. Nelson, C.J. Hansen, C. Akcay, D.A. Ennis, et al., Imposed-dynamo current drive, Nucl. Fusion 52 (083017) (2012) 9.
[2] J. Menard, L. Bromberg, T. Brown, T. Burgess, D. Dix, L. El-Guebaly, et al., Prospects for pilot plants based on the tokamak, spherical tokamak and stellarator, Nucl. Fusion (103014) (2011), 13 pp.
[3] R. Hagenson, R. Krakowski, Steady-state spheromak reactor studies, Fusion Technol. 8 (1985) 1606–1612.
[4] F. Najmabadi, the ARIES Team, The ARIES-AT advanced tokamak, advanced technology fusion power plant, Fusion Eng. Des. 80 (2006) 3–23.
[5] L. Bromberg, M. Tekula, L.A. El-Guebaly, R. Miller, the ARIES Team, et al., Options for the use of high temperature superconductor in tokamak fusion reactor designs, Fusion Eng. Des. 54 (2001) 167–180.
[6] T. Hamp, T.R. Jarboe, B.A. Nelson, R.B. O'Neill, R. Raman, A.J. Redd, et al., Temperature and density characteristics of the Helicity Injected Torus-II spherical tokamak indicating closed flux sustainment using coaxial helicity injection, Phys. Plasmas 15 (082501) (2008).
[7] E. Hooper, R.H. Bulmer, T.K. Fowler, D.N. Hill, H.S. McLean, C.A. Romero-Talamás, et al., Reactor opportunities for the spheromak, In: Current Trends in International Fusion Research: A Review, Washington, DC, March 24-28, 2003.
[11] G. Porter, S. Davies, B. LaBombard, A. Loarte, K. McCormick, R. Monk, et al., Analysis of separatrix plasma parameters using local and multi-machine databases, J. Nucl. Mater. (266–269) (1999) 917–921.
[12] Data table for: Zirconium dioxide [ZrO_2-Y_2O_3 stabilized], http://www.matbase.com (October 2012).
[13] M. Wykes, ITER vacuum pumping systems, 2006 http://cas.web.cern.ch/cas/Spain-2006/PDFs/Wykes.pdf
[14] M. Youssef, Damage rate in V.V. as a function of convective layer thickness, in: APEX Study Memorandum (March 1998), 1998.
[15] K. McCarthy, M. Sawan, D. Sze, M. Tillack, A. Ying, S. Zinkle, Flibe assessment summary, in: APEX Meeting Presentation (November 1998), 1998.
[16] P. Calderoni, P. Sharpe, H. Nishimura, T. Terai, Control of molten salt corrosion of fusion structural materials by metallic beryllium, J. Nucl. Mater. 386–388 (2009) 1102–1106.
[17] T. Nagasaka, M. Kondo, T. Muroga, N. Noda, A. Sagara, O. Motojima, et al., Progress in flibe corrosion study towards material research loop and advanced liquid breeder blanket, in: IAEA FEC Proceedings, 2008, Paper FT/P 2-4.
[18] E. Wallin, Alumina thin films from computer calculations to cutting tools, (Ph. D. Thesis), Linkoping University: Institute of Technology, 2008, Dissertation No. 1221.
[19] A.E. Muhsin, Chemical vapor deposition of aluminum oxide ((Al_2O_3)) and beta iron disilicide (β-$FeSi_2$) thin films (Ph.D. Thesis), University of Duisburg-Essen, 2007 (Ph.D. Thesis).
[20] C.B.A Forty, R.A. Forrest, D.J. Compton, and C. Rayner, Handbook of fusion activation data: Part 1, elements hydrogen to zirconium, AEA FUS 180, May 1992.
[21] T. Hayashi, K. Tobita, Y. Nakamori, S. Orimo, Advanced neutron shielding material using zirconium borohydride and zirconium hydride, J. Nucl. Mater. 368–388 (2009) 119–121.
[22] V. Dostal, M. Driscoll, P. Hejzlar, A supercritical carbon dioxide cycle for next generation nuclear reactors, 2004 (MIT Dissertation).
[23] P. Hejzlar, V. Dostall, M.J. Driscoll, P. Dumaz, G. Poullennec, N. Alpy, Assessment of gas cooled fast reactor with indirect supercritical CO_2 cycle, Nucl. Eng. Technol. 38 (2) (2006).
[24] E. Lahoda, Westinghouse Electric Company, Consulting Engineer, Research and Development: Personal Correspondence (September 2013) (2013).
[25] S. Mylavarapu, X. Sun, J. Figley, N. Needler, R. Christensen, Investigation of high-temperature printed circuit heat exchangers for very high temperature reactors, J. Eng. Gas Turbines Power 131 (2009).
[26] E.I. Administration, Updated capital cost estimates for electricity generation plants, U.S. DOE, http://www.eia.gov/oiaf/beck_plantcosts/pdf/updatedplantcosts
[27] F. Najmabadi, A.R. Raffray, S.I. Abdel-Khalik, L. Bromberg, L. Crosatti, L. El-Guebaly, et al., The ARIES-CS compact stellarator fusion power planet, Fusion Sci. Technol. 54 (2008).
[28] A.S. Corp., Scale-up of second generation HTS wire: 2G-YBCO coated conductor, DOE Peer Review: AMSC 2G Scale-up (July 2004), 2004.
[29] T. Jarboe, Imposed dynamo current drive, 2013 EPR Workshop, http://www.iccworkshops.org/epr2013/uploads/165/epr4talk2013.pdf (February 2013).
[31] F. Dahlgren, T. Brown, P. Heitzenroeder, L. Bromberg, The ARIES Team, ARIES-AT magnet systems, Fusion Eng. Des. 80 (2006) 139–160.
[32] J.E. Rice, A. Ince-Cushman, J.S. deGrassie, L.G. Eriksson, Y. Sakamoto, A. Scarabosio, et al., Inter-machine comparison of intrinsic toroidal rotation in tokamaks, Nucl. Fusion 47 (2007) 1618–1624.
[33] R.L. Klueh, N. Hashimoto, R.F. Buck, M.A. Sokolov, A potential new ferritic/martensitic steel for fusion applications, J. Nucl. Mater. 283–287 (2000) 697–701.
[34] S. Zinkle, UT/ORNL Governor's Chair, Dept. of Nuclear Eng. and Dept. of Mater. Science, University of Tennessee, Personal Correspondence (March 2014).
[35] B.S. Victor, T.R. Jarboe, C.J. Hansen, C. Akcay, K.D. Morgan, A.C. Hossack, and B.A. Nelson, Sustained spheromaks with ideal n = 1 kink stability and pressure confinement, Physics of Plasmas, submitted for publication.

Please cite this article in press as: D.A. Sutherland, et al., The dynomak: An advanced spheromak reactor concept with imposed-dynamo current drive and next-generation nuclear power technologies, Fusion Eng. Des. (2014), http://dx.doi.org/10.1016/j.fusengdes.2014.03.072